NASA CR-132459

The Effect of Simulator Dynamics on Pilot Response

EARL F. WEENER

National Aeronautics and Space Administration
Contract No. NSR 23-005-364 by

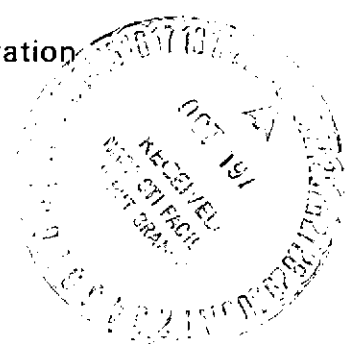

Department of Aerospace Engineering

NASA CR-132459

THE EFFECT OF SIMULATOR DYNAMICS ON PILOT RESPONSE

By Earl F. Weener

Prepared under Contract No. NSR 23-005-364 by
the Department of Aerospace Engineering
THE UNIVERSITY OF MICHIGAN
Ann Arbor, Mich.

for

NATIONAL AERONAUTICS AND SPACE ADMINISTRATION

ABSTRACT

THE EFFECTS OF VISUAL FLIGHT DISPLAY DYNAMIC LAGS ON THE TRACKING PERFORMANCE IN A FIXED-BASE FLIGHT SIMULATOR

by

Earl F. Weener

This report presents the results of an experimental study of the effects of visual display dynamics on the altitude tracking performance of a subject in a fixed-base flight simulator. The subject, flying the linearized longitudinal equations-of-motion, attempted to maintain the same altitude as two airplanes positioned three-hundred feet ahead, as in level formation flying. The horizon together with the two leading aircraft were represented symbolically on a CRT display. The subject's aircraft was disturbed by atmospheric turbulence. Various bandwidths of second-order dynamics were interposed between the true aircraft altitude and the displayed altitude; no dynamics were interposed in the attitude display. Experiments were run using two experienced pilots and two substantially different longitudinal dynamics for the piloted aircraft.

The data indicate a relationship between the bandwidth of the display dynamics and the short-period characteristics of the simulated airplane. For an airplane with a relatively fast pitch response (short-period natural frequency of 4.8 radians/second and damping ratio of 0.38) the presence of altitude display dynamics with a bandwidth as

high as five times the short-period natural frequency caused significant degradation of altitude tracking performance. However, for an aircraft with slower pitch response (short-period frequency of 2.6 radians/second and damping ratio of 0.54) the presence of the display dynamics had no significant effect until the bandwidth was approximately twice the short-period natural frequency.

ACKNOWLEDGMENTS

The author wishes to express his appreciation for the suggestions and assistance offered by Dr. R. M. Howe, Dr. R. W. Pew, and Dr. L. E. Fogarty throughout the investigation.

The digital computer programing assistance of Mr. Roger Metzler is greatly appreciated.

The author also wishes to thank Mr. John Hanson and Mr. Elliot Freeman, the pilot/subjects, for their participation.

This research was sponsored in part by the National Aeronautics and Space Administration under Contract NSR-23-005-364.

TABLE OF CONTENTS

LIST OF FIGURES

LIST OF TABLES

1.0 INTRODUCTION

1.1 Background

Both fixed-based and moving-base simulators are often used to simulate flight by visual reference to objects outside of the cockpit. In many installations these visual displays are generated by a multiple-degree-of-freedom TV camera which moves with respect to a scale model. Although the rotational motions of the servos driving the TV camera normally exhibit satisfactorily high dynamic response, this is not necessarily true for the translational servos. In particular, the servo drive for the z-axis (vertical axis for an airplane in level flight) may exhibit appreciable dynamic lags in its response to translational motion commands.

Figure 1.1 shows a simple conceptualization of the system. The camera-drive system introduces both linear and nonlinear dynamic effects into the display. The physical hardware can present nonlinearities such as thresholds, deadzones, limiting, and friction. Generally, these effects are minimized by proper hardware design. The effects of some of these nonlinearities were reported by Barnes (Ref 1). He found that the primary effects were degradation of control accuracy and production of low frequency pilot-induced oscillations or limit cycles.

The small-signal frequency response of the camera drive system is another important characteristic. In this case, the servo-drive input can be at least partially corrected by suitable pre-filtering of

the servo-drive input signals with a filter having the inverse frequency response of the servo. The small-signal servo dynamics can be reasonably approximated by a linear second order system with a damping ratio in the neighborhood of 0.7. The bandwidth of the servo-drive system becomes an important design specification.

This report presents the results of a study of the effects of vertical-axis translational-servo bandwidth on the tracking performance of a pilot in a rudimentary fixed-base flight simulator.

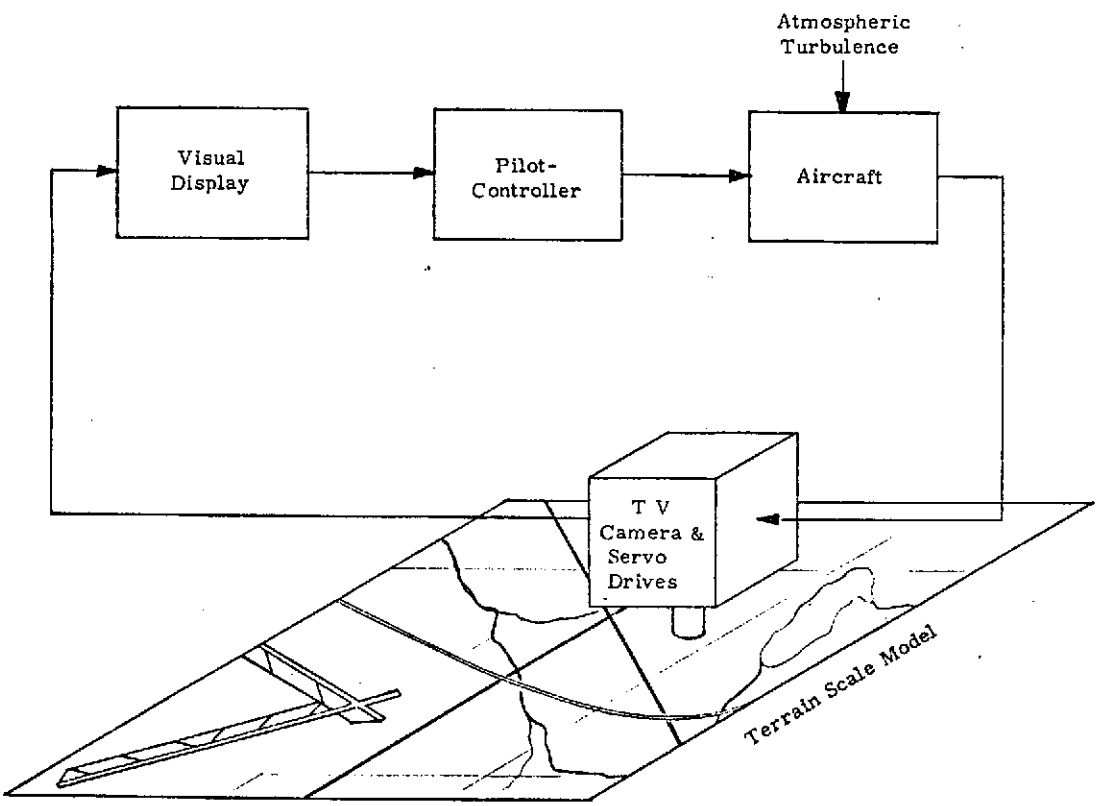

Figure 1.1 Simple conceptualization of a flight simulator with a visual display system

1.2 Description of the Experiment

The principle question of interest is the following: how good must the z-axis translational servo dynamics be in order to present to the pilot a visual simulation which will be a useful representation of the real motions of the counterpart aircraft? To answer this question, a rudimentary fixed-base flight simulator was devised. The pilot flew airplane longitudinal equations-of-motion solely by reference to a computer generated CRT visual display. A formation flying task was utilized, since in this task the displayed altitude (inertial z-axis position) was of primary concern to the pilot. He attempted to maintain the piloted airplane at the same altitude as the lead aircraft in the presence of atmospheric turbulence. The inside-out display presented only pitch angle and altitude deviation away from nominal.

Simulated display dynamics were interposed between the true altitude deviation of the "airplane" and the displayed altitude deviation. The natural frequency of the display dynamics was systematically varied over a range of frequencies. The index of performance was the pilot's mean-square error in maintaining proper altitude in the presence of the simulated turbulence. Two airplanes with substantially different short-period longitudinal characteristics were simulated to determine some of the interactions between the display dynamics and the airplane dynamics.

1.3 Organization of the Report

For the reader who is primarily interested in the conclusions, Section 5 contains the pertinent definitions and data, and Section 6 discusses the resulting conclusions. Some suggestions for further research are also presented in Section 6. Section 4 is recommended for the reader who is also interested in how the experiment was organized and conducted. The preliminary experiment and data are described in Section 3. Specific details of the simulation, display, display dynamics, disturbance-input generation and data acquisition are contained in Section 2, and Appendices A and B.

2.0 SIMULATION AND EQUIPMENT

The simulation is shown in block diagram form in Figure 2.1. The configuration is similar to the conventional arrangement for a tracking or regulation task except for the additional dynamics present in the altitude feedback path. These additional dynamics represent visual display-generation hardware which has both inertia and damping in translational motion. The computer-generated CRT visual display presented both pitch angle and altitude deviation to the pilot. The tracking task was a simplified formation flying task. The subject attempted to maintain an in-trail position at the same altitude as the two lead aircraft, while flying through a turbulent atmosphere.

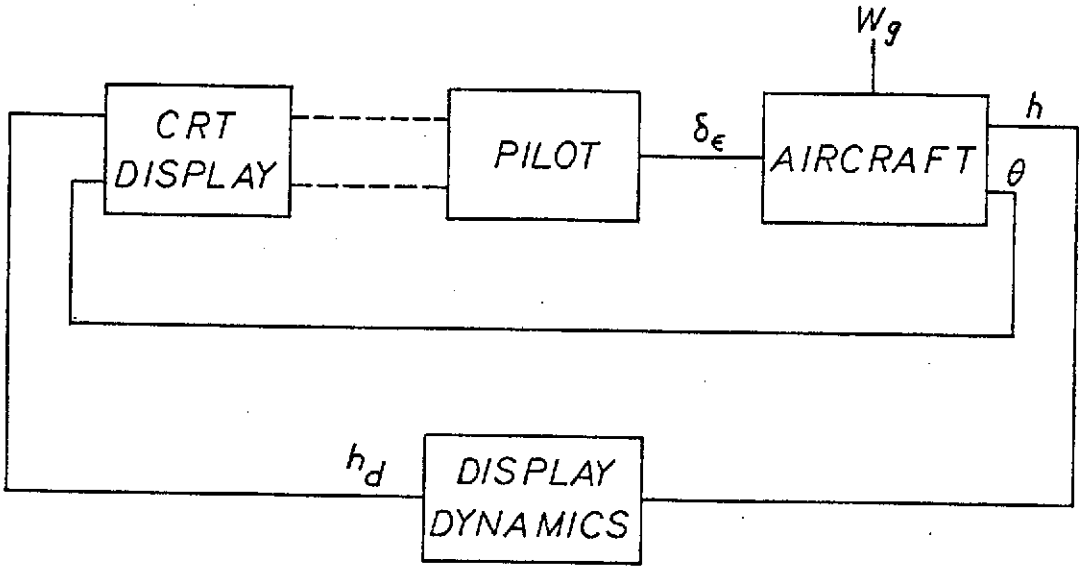

Figure 2.1 Simulation block diagram

This chapter deals with the mechanics of the simulation. Section 2.1 discusses the visual display. Details of the experiment room lay-out are contained in 2.2. The vehicle simulation is detailed in Section 2.3. Section 2.4 contains details of the disturbance input or vertical turbulence generation, and data acquisition is discussed in section 2.5.

2.1 Visual Display

The pilot controlled the simulated aircraft solely by reference to the visual display; there was no cockpit instrumentation. A 19" x 14" (48 cm x 35 cm) rectangular CRT displayed a visual horizon line and two aircraft symbols. Four different typical scenes are shown in Figure 2.2. Displacement of the horizon from center showed the piloted-aircraft pitch angle. The pitch angle was displayed as a true-scaled angle and had a $\pm 13^{\circ}$ maximum deviation. The displacement of the triangular delta wing airplane symbols from the horizon line indicated the altitude deviation away from nominal. The nominal condition is shown in Figure 2.2.c and is simply level flight at the same altitude as the two lead aircraft. The display was an inside-out display; in other words, the scene moved in the same manner as it would have if the pilot were looking out the front window of the cockpit.

The display also included aspect changes for the two leading aircraft. If the aircraft were below nominal altitude but flying level,

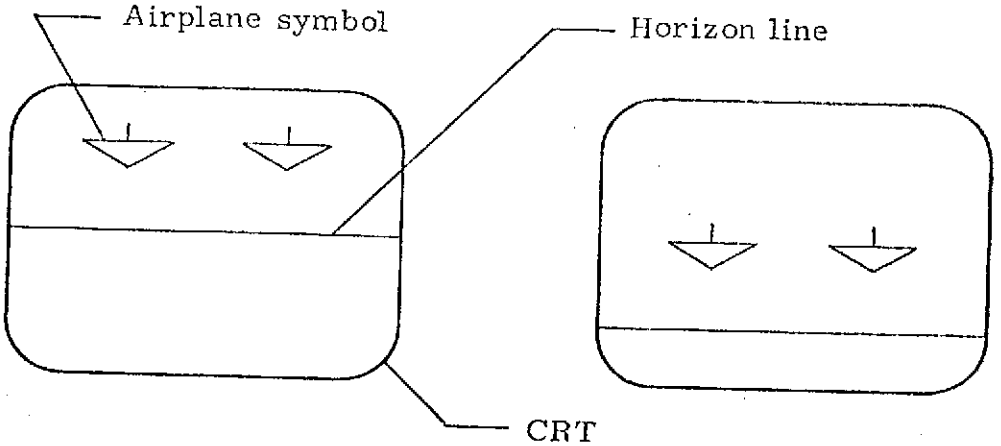

(a) Level flight below nominal altitude

(b) Pitch-up, nose-high attitude

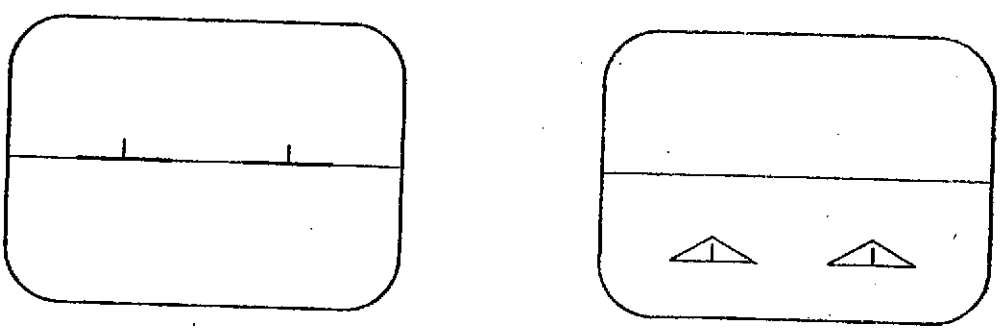

(c) Level flight at nominal altitude

(d) Level flight above nominal altitude

Figure 2.2 Typical visual display scenes

the two aircraft symbols would appear as blunt arrow heads pointing downward toward the horizon line, similar to that shown in Figure 2.2.a. This aspect resembles that which a pilot would see in flight if he were behind and under a delta wing airplane. A quick pitch up is shown in Figure 2.2.b; the piloted airplane has not yet started to climb to the nominal altitude. Finally, Figure 2.2.d shows the piloted-aircraft in level flight, but above the altitude of the two lead aircraft. The size of the aircraft symbols remained constant, which is consistent with the assumption that the piloted aircraft always stayed 300 feet behind the two lead aircraft.

The altitude of the lead aircraft was not disturbed; however the piloted aircraft was perturbed by a simulated vertical gust spectrum. The effects of the vertical turbulence on the displayed scene were manifested in changes in pitch angle and a vertical or heave motion.

The display was generated by the analog and logic sections of the hybrid computer. The sweep and update rates of the display were high enough to prevent flicker.

2.2 Experiment Room

The subjects flew the simulation in a small room in the University of Michigan Simulation Center. The windows were covered to reduce peripheral disturbances. Figure 2.3 shows a photograph of the subject's chair, side stick controller, and the CRT display. Pertinent dimensions are shown in Figure 2.4.

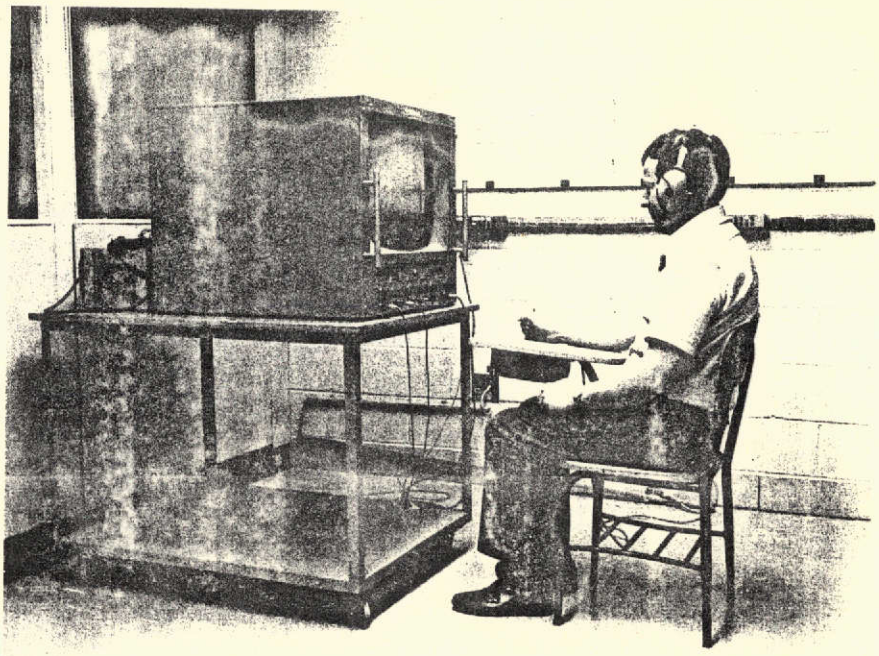

Figure 2.3 Subject and display setup

The control stick was mounted on the subject's chair and was operated with the right hand. The 6 1/2 inch (16.5 cm) long stick had a full angular deflection of $\pm$ 40 degrees. The restoring spring constant was 0.34 ft-lb/radian. A damped second order approximation of the control stick would have the following coefficients:

natural frequency = 78.5 radian/sec

damping ratio = 0.02.

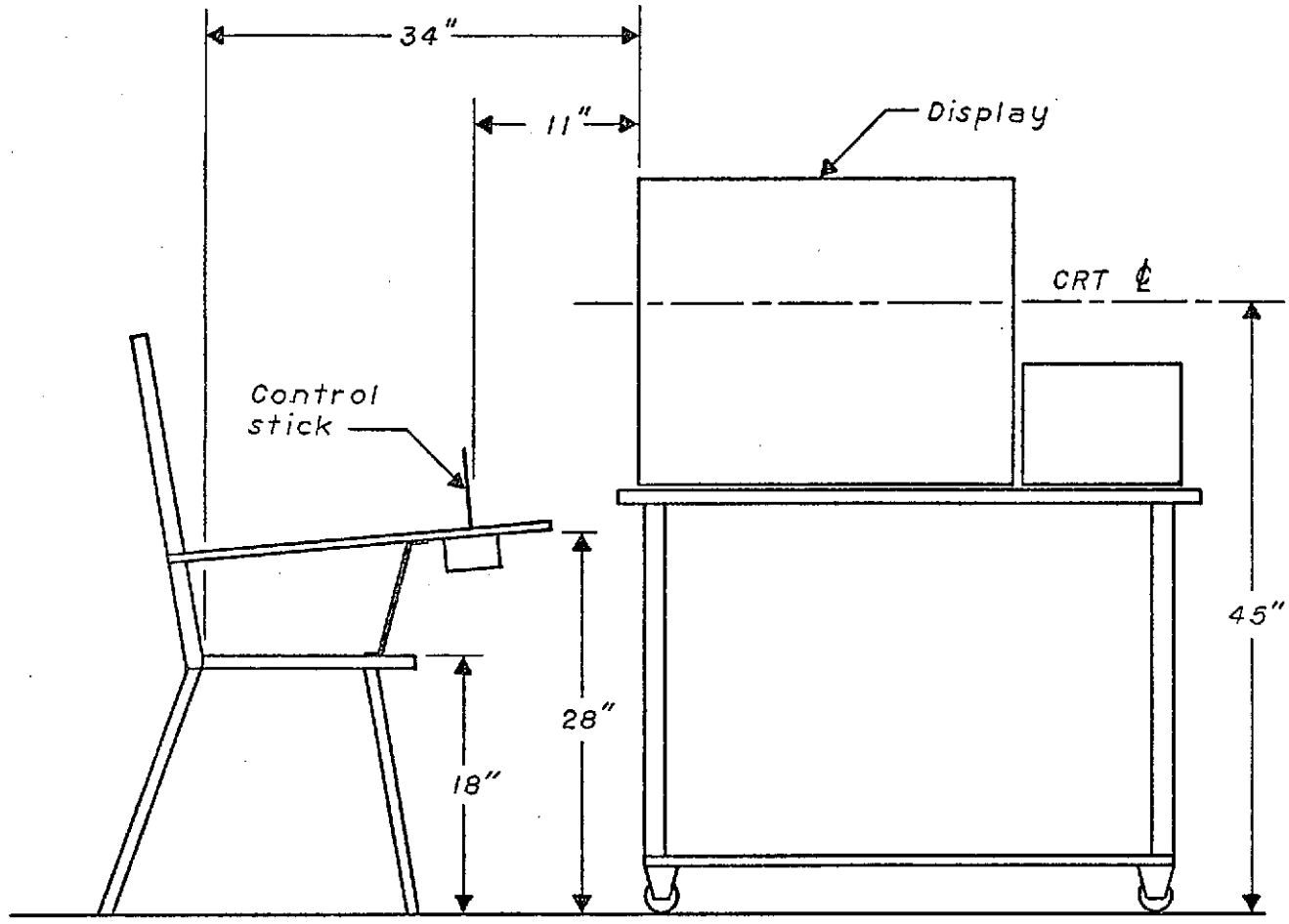

Figure 2.4 Pertinent dimensions of experimental setup

The subject was seated so that his eyes were level with the center of the CRT at a distance of 30 inches (76 cm) from the screen. This corresponded to a simulated distance of 300 feet behind the lead aircraft. The maximum altitude deviation displayed on the CRT then corresponded to 120 feet of vertical travel.

2.3 Computer Simulation of the Aircraft

Appendix A gives the linearized longitudinal equations-of-motion that were mechanized on the Simulation Center's Applied Dynamics AD 2-64-PB Hybrid Computer. This computer also controlled both the run timing and the CDC 160A digital computer, which was used for on-line digital recording of the runs.

In this section the general simulation and equipment is discussed. The following subsection deals with the display dynamics.

2.3.1 Display Dynamics

The variables displayed to the pilot were the pitch angle and the altitude deviation. As mentioned previously, the displayed altitude deviation, h_d, was in general not the same as the computed aircraft altitude deviation, h. The display dynamics, shown in Figure 2.5, were modeled as a second order underdamped system. The damping ratio, ζ_d, was held constant at $\zeta_d = 0.707$. The natural frequency of the display dynamics, ω_{n_d}, was the primary experimental parameter.

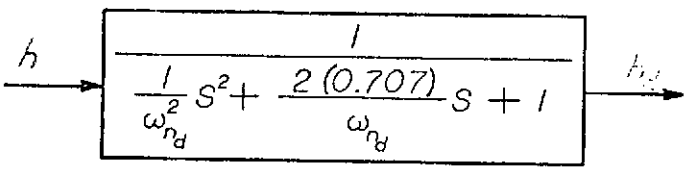

Figure 2.5 Display dynamics approximation

2.3.2 Aircraft Simulation

To determine some of the interactions between the aircraft dynamics and the display dynamics when a human operator is present in the loop, two airplanes with substantially different short period dynamics were simulated. The airplane longitudinal dynamic characteristics are tabulated in Table 2.1.

Aircraft	Short period		Phugoid	
	ω_{sp}	ζ_{sp}	ω_p	ζ_p
1	4.8 r/s	0.38	0.07 r/s	0.09
2	2.6 r/s	0.54	0.11 r/s	0.06

Table 2.1 Airplane longitudinal dynamic characteristics

The aircraft equations of motion in state-space form, are given in Appendix A. Although the phugoid characteristics of the two aircraft are somewhat different, the phugoid dynamics have relatively little effect on the control task. On the other hand the short period characteristics differ considerably with the result that aircraft #1 has a much quicker response to rapid changes in control input than does aircraft #2.

In terms of longitudinal handling qualities, aircraft #1 would rate a poor pilot opinion, whereas aircraft #2 would rate a satisfactory pilot opinion as shown in Figure 2.6 (Ref. 2). Subject comment throughout the experiment favored aircraft #1 however. The inversion of handling quality pilot opinion between inflight data and the subject comment probably can be explained by

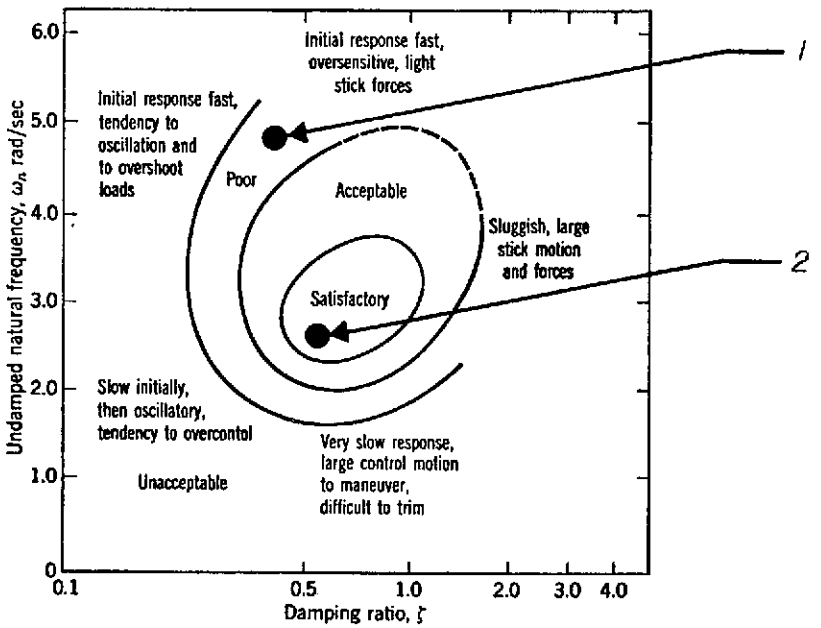

Figure 2.6 Longitudinal short-period pilot opinion contours

the fact that this was a fixed base simulation. Hence,the subjects had neither vestibular nor kinesthetic cues and for this reason did not experience the normal load factors which would be generated by abrupt pitch-up or pitch-down motions.

For airplane #1, the normal accelerations would have presented an inhibiting influence on the subject's control inputs. In flight, the rapid response of this airplane would have produced a fairly uncomfortable ride had it been flown in the same way in which it was flown in the fixed-base simulation. Airplane #2 had a lower natural frequency and higher damping in the short period mode and the high normal accelerations characteristic of airplane #1 would not have been generated in flight. Hence, the lack of motion did not alter the subjects control philosophy from the in-flight philosophy as much as it did in the case of Airplane #1. In this tracking task the subject's error score was decreased if he corrected the effects of the turbulence as rapidly as possible. After each run the subject was informed of his error score for that run. Since the subject did not have to be concerned with load factors, he would concentrate on the airplane's flight path only. In the case of airplane #1, he could, in fact, elicit very rapid responses. Consequently, the subjects favored the response of airplane #1 over that of airplane #2. Even when display dynamics were present in the altitude feedback loop, the subjects still favored airplane #1 over airplane #2.

The elevator coefficients for the two airplanes were adjusted so that the control-stick gains in the region of closed loop system cross-over frequency were approximately equal. Figures 2.7 and 2.8 show the longitudinal frequency response for pitch angle, θ, and true altitude, h, with elevator input, δe; $Y_{\theta}{}_{\delta e}$ and $Y_{h}{}_{\delta e}$, respectively. As can be seen, the gains in the region between the phugoid peak and the short-period knee are very nearly equal.

In the simulation, the only elevator input was $C_{m\delta_e}\,\delta e$. All other elevator position and rate coefficients were neglected because of their small effects.

2.4 Disturbance Input

The pilot/subject in this simulation attempted to keep the piloted aircraft at the nominal altitude, behind the two lead aircraft, in the presence of atmospheric turbulence. The pilot did not track the turbulence, but instead attempted to suppress the effects of it; hence the task was not that of tracking, but rather, that of regulating. This turbulence was generated by suitable analog filtering of pseud-random binary noise.

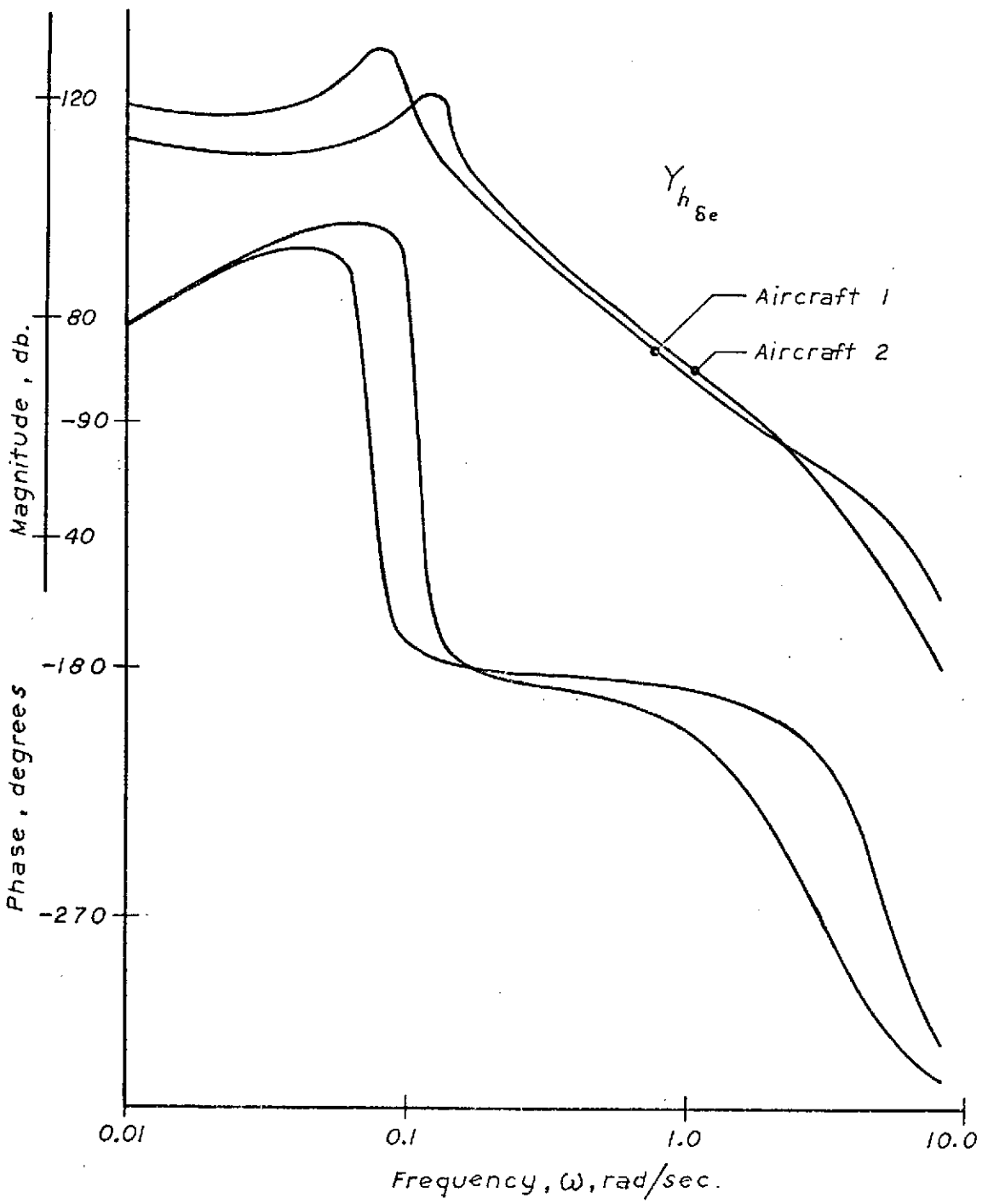

Figure 2.7 Phase-Magnitude plot for elevator to altitude transfer function

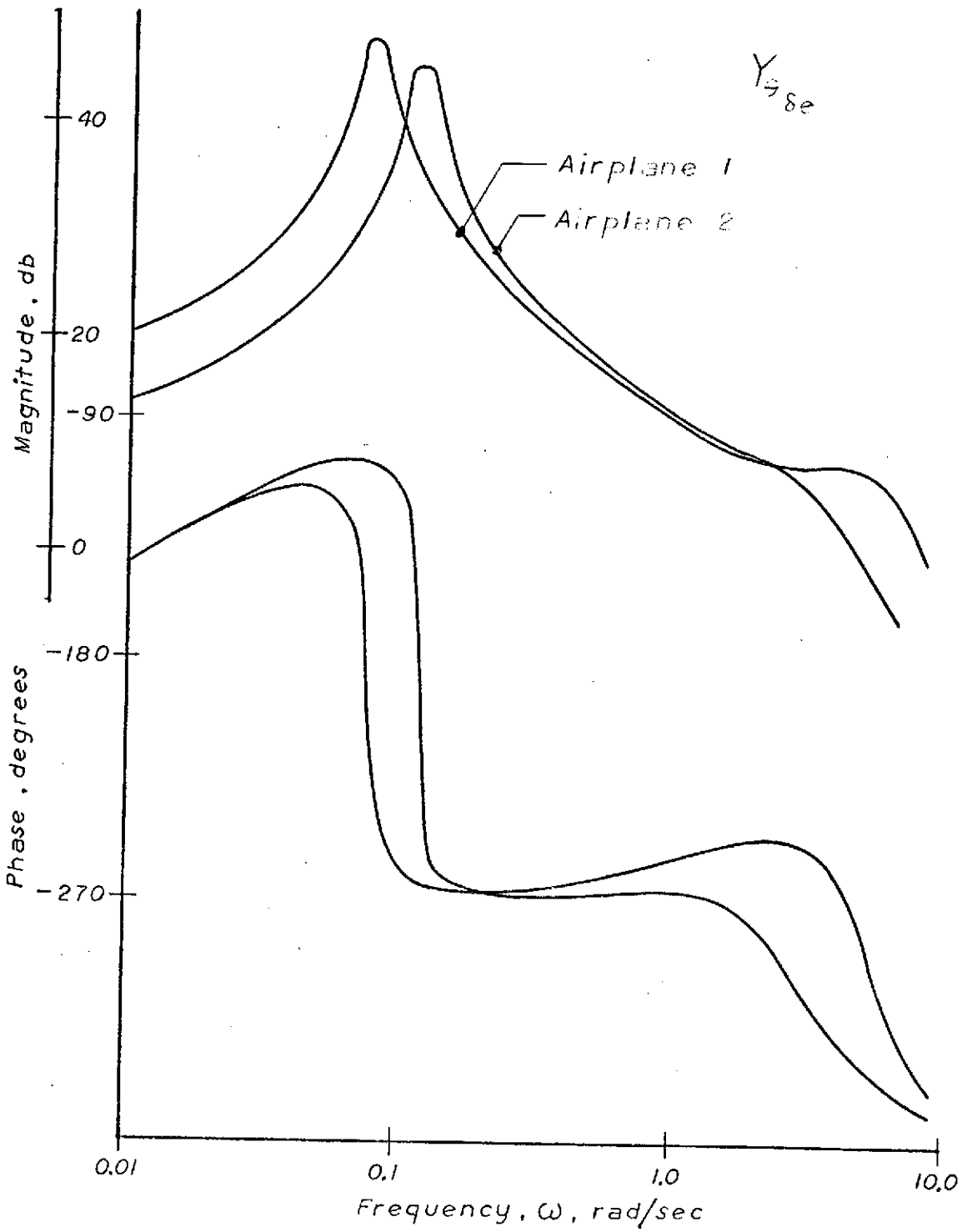

Figure 2.8 Phase-Magnitude plot for elevator to pitch angle transfer function

Turbulence is an atmospheric phenomenon which can be represented at a point by three mutually orthogonal velocity components, all of which are functions of time. However, turbulence is a random process which cannot be described as an explicit function of time, and as such, a statistical-probabilistic approach is easiest to work with. We can assume that turbulence can be respresented by a Guassian or normally-distributed random process. Another assumption almost universally made is that the process is stationary and ergodic. At high altitudes we can also assume that turbulence is isotropic or independent of the coordinate system which is used to describe it. Finally, we assume that the aircraft speeds are large compared to the turbulence velocities and their rates of change. This amounts to neglecting the time dependence and treating turbulence as a pattern frozen in space. This assumption is known as "Taylor's hypothesis."

In this simulation of longitudinal dynamics we need not be concerned with lateral turbulence, but only with longitudinal and vertical turbulence velocities. A further simplification can be made. The open loop response of the airplane to longitudinal gusts or turbulence is primarily in the low frequency region up to and including the phugoid frequency region. When the human operator closes the loop around the airplane, he generally controls low frequency disturbances with the elevator, acting as a gain on the pitch-angle error. Hence,the effects of longitudinal turbulence are negligible for this simulation;

consequently, this component of turbulence has been disregarded.

The remaining disturbances are due only to the vertical-gust spectrum. The main effects are a vertical heave and a pitching motion. The principal contribution to the heave motion is due to the change in angle-of-attack of the wing; hence, the aircraft experiences a change in the vertical force or lift. Similarly, the change in angle-of-attack of the aircraft causes a change in the pitching moment due primarily to the horizontal stabilizer. The smaller wing contribution to the pitching moment is dependent on the center-of-gravity location.

As stated previously, vertical turbulence can be visualized as a field of various vertical wind velocities frozen in space. In the frequency domain this random process can be described by a spectral power distribution. Two widely accepted models of turbulence spectra are the von Karman spectrum and the Dryden spectrum (Ref 3), both shown in Figure 2.9. The Dreyden spectrum can be implemented with reasonable accuracy by suitable analog filtering of a white noise source. The approximation to the Dreyden spectrum utilized in this simulation is shown in Figure 2.10. The break frequencies chosen were 1 rad/sec and 10 rad/sec. This corresponds to a characteristic gust wavelength, L, of 1160 ft with a flight velocity of 862 ft/sec.

The small circles on Figure 2.10 represent the average power spectral density of five distinct two minute runs. These spectrum

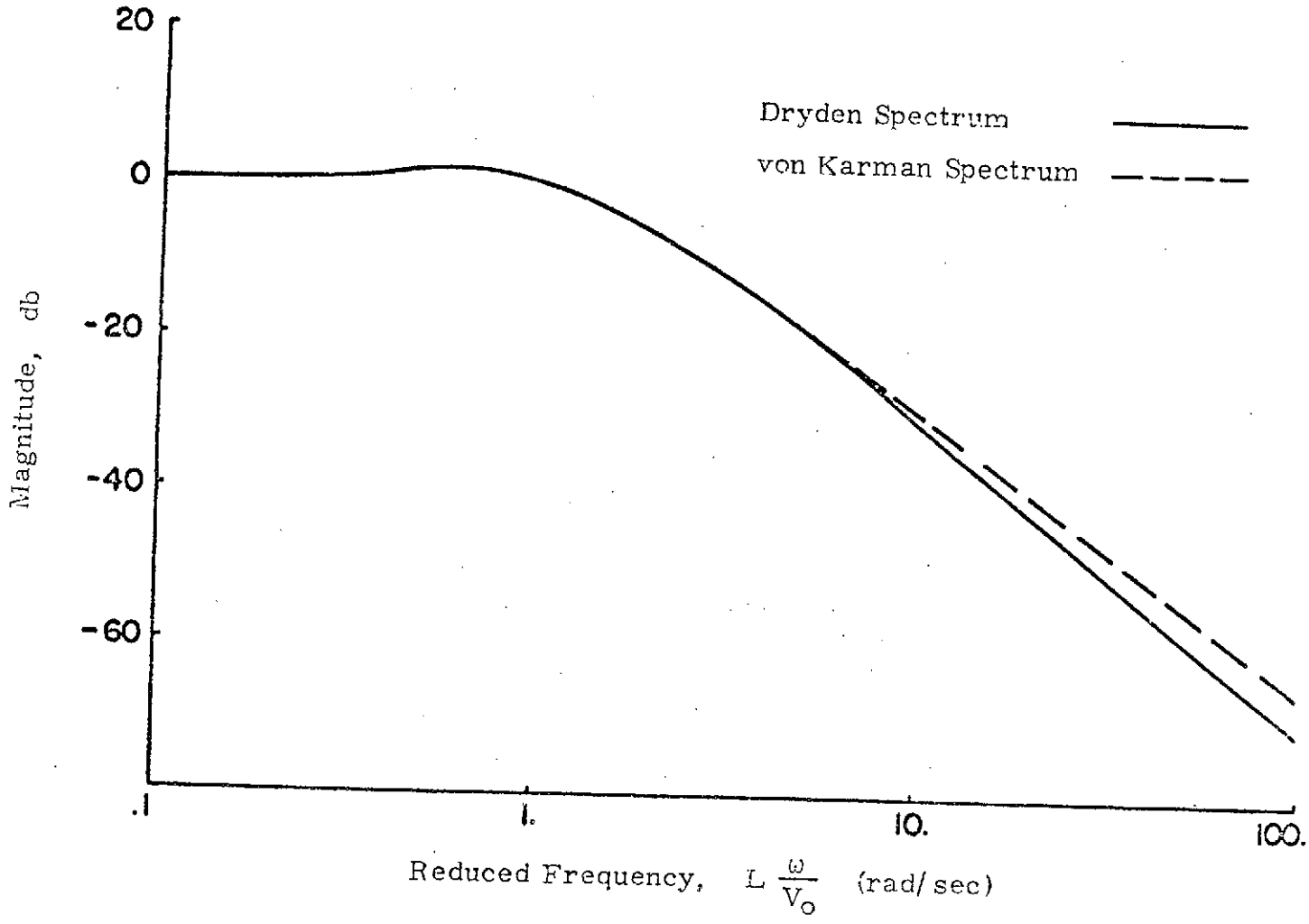

Figure 2.9 The Dryden and von Karman spectral models

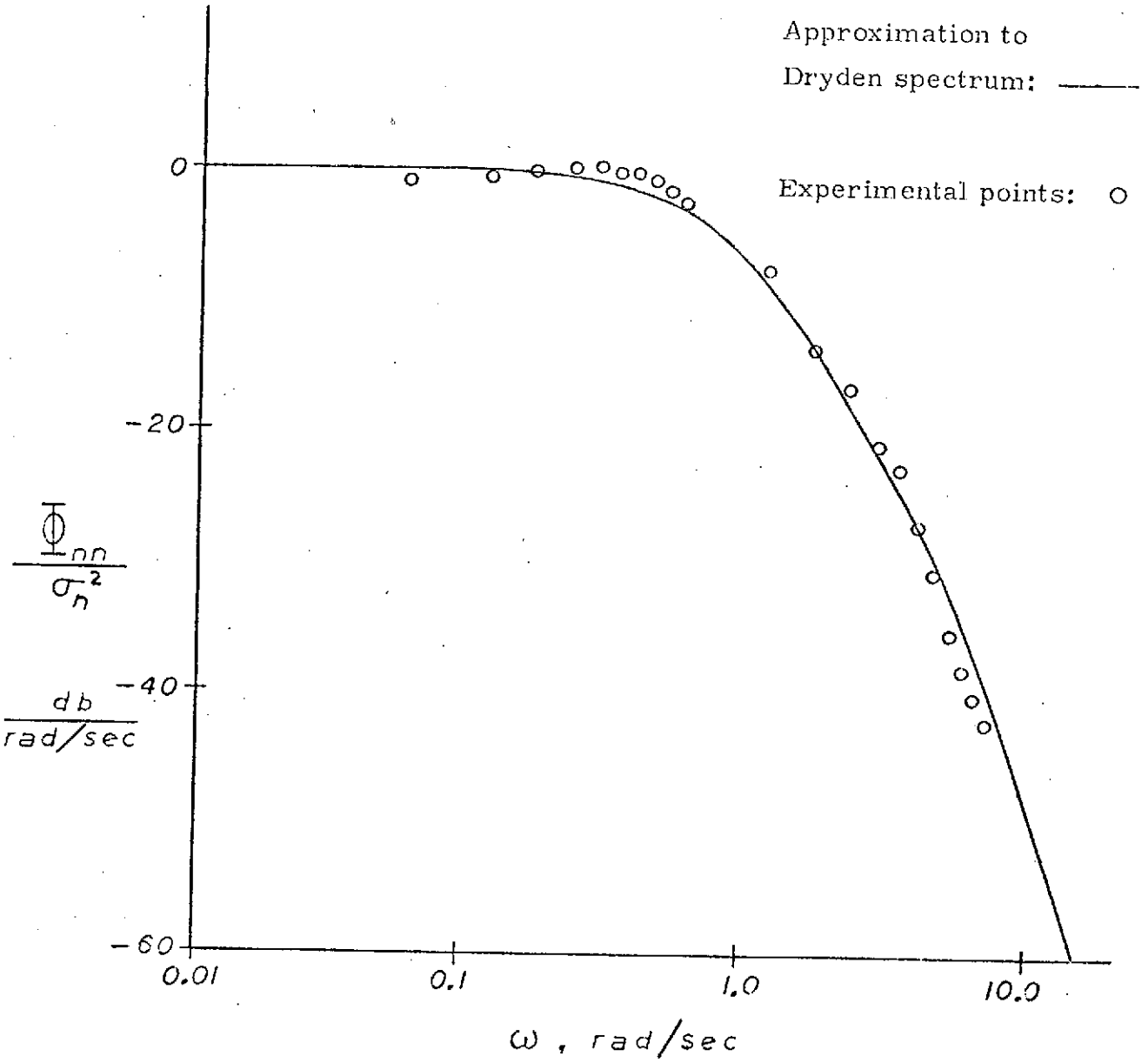

Figure 2.10 Approximation to Dryden spectrum with experimentally obtained sample spectrum

were calculated using the equipment and processes described in the following section (2.5).

The distrubance input to the airplane was the angle-of-attack variation,

$$\Delta\alpha(t) = \frac{W_g(t)}{V} = \frac{\text{Vertical gust velocity}}{\text{Aircraft nominal velocity}}$$

and the rate of change of $\Delta\alpha$,

$$\dot{\Delta\alpha}(t) = \frac{d}{dt}\,\Delta\alpha(t) = \frac{1}{V}\,\frac{d}{dt}\,w_g(t)$$

due to the vertical turbulence. The vertical gust velocity used in the simulation was generally in the neighborhood of 5 ft/sec (1.5 meter/sec) R.M.S.

Due to the idiosyncratic nature of pseudo random binary noise generation the optimal relationship between the noise generator clock frequency and the two break frequencies of the following analog filters was not well defined. Results of tests of the amplitude distributions at several different clock frequencies are given and discussed in Appendix B.

2.5 Data Acquisition

Two fundamentally different types of data were recorded. The mean-square altitude deviation and the mean-square vertical gust velocity were integrated for each experimental run. These two integral mean-square numbers were recorded at the end of each run and were used to define a relative performance index(which is discussed in the following chapters).

The second type of data acquired consisted of on-line digital

recordings of several of the input and state variables. A Control Data CDC 160A/CDC 8000 digital computer sampled the various input lines at a rate of 40 samples per second, digitized and recorded the corresponding numbers on seven track magnetic tape. For the first subject, eight inputs and state variables were sampled and recorded. However, since several of these variables are analytically related, four redundant variables were eliminated from the recordings of the second subject. The four basic variables recorded in both cases were:

angle-of-attack noise input

elevator input

displayed altitude deviation

pitch angle.

Statistical and frequency analysis of this data was performed at The University of Michigan Computing Center on an IBM-360-67M, and is described in the following chapters.

3.0 PRELIMINARY INVESTIGATION

A preliminary experiment was performed to obtain a general idea of the effects of display dynamics on altitude tracking performance. A wide range of display-dynamics natural frequencies was examined for a limited number of replicates. This chapter describes this preliminary experiment and the resulting data.

A series of forty experimental runs was made with display-dynamics natural frequencies ranging from 3 radians/second to 30 radians/second. Somewhat uniformly interspersed among the forty runs were fifteen runs without display dynamics. These runs were utilized to establish a control condition. At the beginning of each run the subject was generally unaware of the presence or absence of display dynamics.

The airplane simulated was airplane #1, the aircraft with the higher natural frequency and lower damping ratio in the short-period mode. The disturbance input was pseudo-random binary noise filtered by a single-stage low-pass filter with a first order roll-off frequency of 1/2 radian/second. The amplitude of the disturbance input resembled mild turbulence. This input spectrum differs from the vertical gust spectrum used in the later, more extensive, experiment. The subject (author Weener) in this preliminary experiment was an experienced general aviation pilot.

Approximately three runs of two-minute duration were made at each of the eight different display-dynamics natural frequencies. For each run, the mean-square altitude deviation and mean-square disturbance input were measured and used to define a relative Mean-Square Tracking Error, MSTE:

$$\text{MSTE} = \frac{\text{MS altitude deviation}}{\text{MS disturbance input}}$$

For each display dynamics configuration these MSTE scores were averaged and then normalized by the average MSTE scores for the no-dynamics control runs. This normalized mean-square score is the ratio of the average MSTE score for a particular display dynamics configuration to the score without display dynamics and will be designated henceforth in this report as the Performance Ratio, PR.

$$\text{PR} = \frac{\text{average MSTE with dynamics}}{\text{average MSTE without dynamics}}$$

The PR represents the fractional increase in the mean-square tracking error due to the presence of the display dynamics.

Figure 3.1 shows the resulting PR vs display-dynamics natural frequency for the preliminary data. For frequencies below 15 radians/second the performance ratio, PR, increases almost exponentially as the display-dynamics natural frequency decreases. For display natural frequencies above 15 radians/second the effect of the display dynamics was negligible.

In many of the runs with display dynamics the subject could not

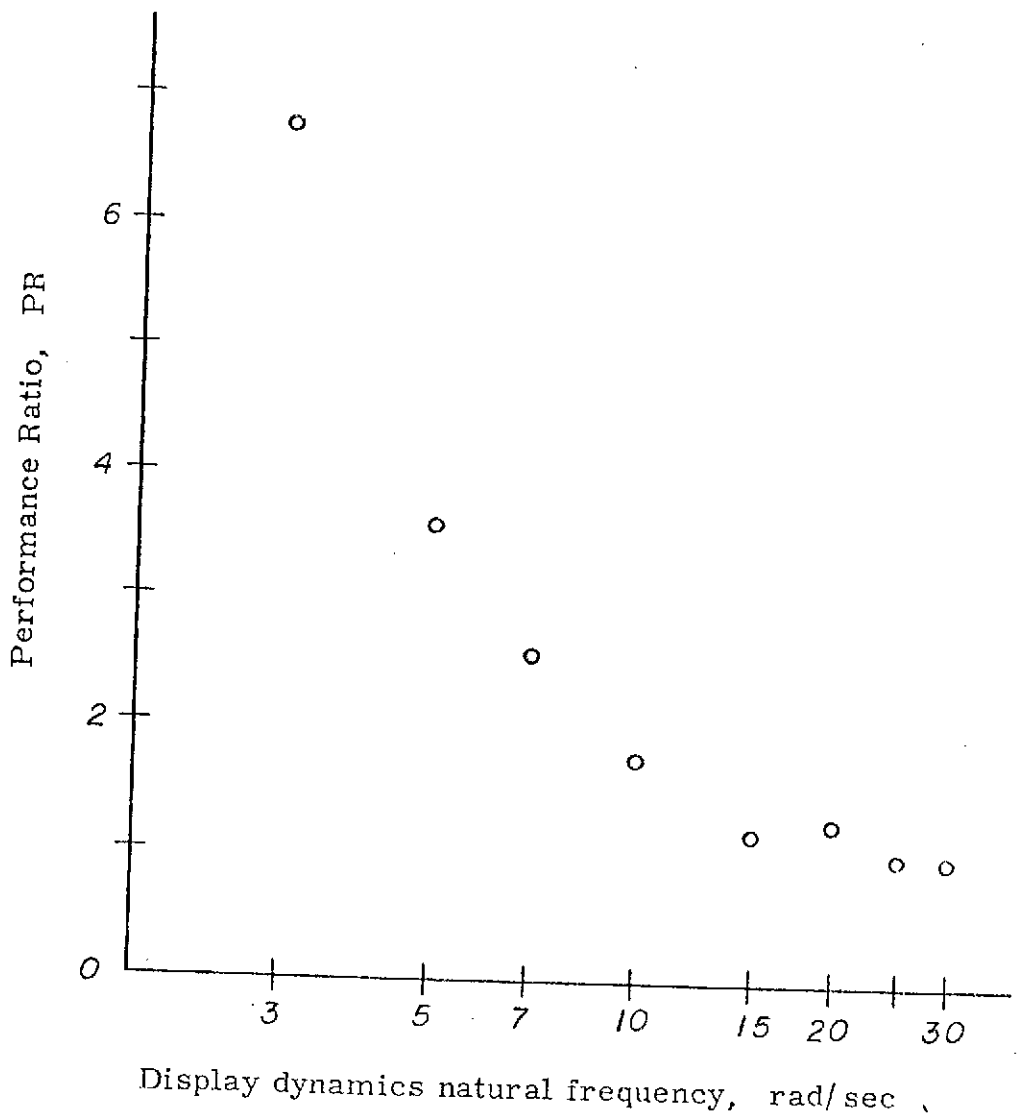

Figure 3.1 Preliminary data— Performance Ratio v. s. display dynamics natural frequency

reliably identify the presence of display dynamics, and yet his error score or PR was significantly greater than 1. Only for the lowest values of display-dynamics natural frequencies could he identify the dynamics with any degree of confidence. This was primarily due to the tendency of the subject to oscillate about the nominal altitude in a limit cycle when the display natural frequency was low. This low-frequency limit cycle is similar to that due to visual display thresholds reported by Barnes (Ref 1).

In summary, the preliminary data was obtained for only one airplane controlled by a non-naive subject. However, the results based on a limited number of replicates were essentially substantiated in the subsequent, more extensive experimental effort.

4.0 THE EXPERIMENT

In any research involving a human operator in the loop the experiment must be designed carefully, since the human operator is capable of learning, adaptation, and optimization; or in control terminology, he possesses non-stationary behavior. Consequently, the various experimental variables must be arranged so that extraneous effects and interactions can be reduced as much as possible. The following section (4.1) deals with the matrix of experimental conditions and the sequential arrangement of these conditions to achieve as much of a properly balanced experiment as possible. Section 4.2 describes the subjects' background and briefing. The experimental procedure is described in section 4.3.

4.1 Design of the Experiment

The results of the preliminary experiment indicated that the display-dynamics frequency range of interest was below 25 radians/second. Above 25 radians/second the degradation of tracking due to display dynamics was negligible. The physical display-generation hardware on which this simulation study is based has a lower limit of dynamic response comparable to a second order system with a natural frequency of 3 radians/second and a damping ratio of 0.707. Consequently, tracking performance with display dynamics in the range of 3 radians/second to 24 radians/second was examined and compared to control runs with no display dynamics. Five different

display natural frequencies together with the control condition of no dynamics constitute the six display-dynamics configurations.

As discussed in Section 2.3.2, two different airplanes were simulated to determine the interaction of the aircraft short-period dynamics with the display dynamics. The matrix of 12 different experimental conditions is shown in Figure 4.1. These 12 conditions were arranged in an order which was designed to reduce the effects of the sequence of display dynamics and aircraft, and the interaction between aircraft, fatigue, learning, and display dynamics. The order of experimental conditions for each subject is listed in Table 4.1. Each of these twelve conditions comprised fifteen replicates. The data were taken during six separate sessions with two experimental conditions per session.

4.2 Subject Background and Briefing

The two subjects utilized in the major study were both experienced pilots. Subject #1 had both fixed-wing and rotary-wing experience; subject #2 had only fixed-wing experience. A summary of their flight experience is given in Table 4.2.

Both subjects were briefed informally on the general aims of the experiment. They were told that there were two airplanes, and that there might be inaccuracies in the simulated visual display. All questions were answered as completely as possible except

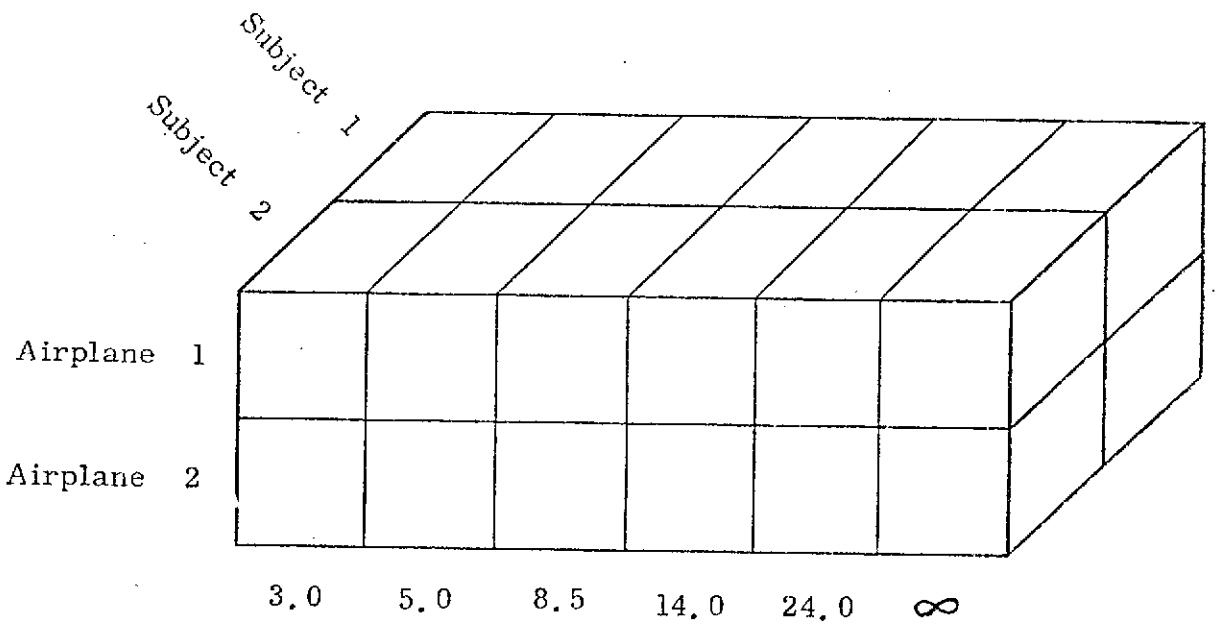

Figure 4.1 Matrix of experimental conditions

day	subject 1			subject 2		
	condition			condition		
	1st	2nd	aircraft	1st	2nd	aircraft
1	∞	8.5	1	∞	8.5	2
2	5.0	24.0	2	5.0	24.0	1
3	14.0	3.0	1	14.0	3.0	2
4	3.0	14.0	2	3.0	14.0	1
5	24.0	5.0	1	24.0	5.0	2
6	8.5	∞	2	8.5	∞	1

Table 4.1 Order of experimental conditions for each subject

Subject 1

Military experience

250 hr fixed-wing light aircraft
200 hr fixed-wing transport aircraft
1500 hr rotary-wing aircraft

Subject 2

Civilian experience--scheduled airline

800 hr fixed-wing light aircraft
4000 hr fixed-wing transport aircraft

Table 4.2 Summary of subjects' flight experience

those relating to the display dynamics. They were asked to fly the simulated airplane in a manner as similar to a real airplane as possible. Following the briefing, each subject was allowed six practice runs in each of the two airplanes, but without display dynamics. The separate orientation session was held prior to any data-taking sessions. Each of the six subsequent sessions comprised two different experimental conditions, both with the same airplane. For each experimental condition, prior to recording any data, the subject was allowed several 2 minute runs with and without turbulence input to familiarize himself with the particular airplane-display configuration. These warmup runs generally allowed the subject to adapt to the experimental condition before any data were recorded.

4.3 Experimental Procedure

The following material deals with operational details of the sessions during which data were recorded.

Prior to each experimental session, fairly extensive static checks and calibrations were performed and recorded. In addition, a dynamic calibration was performed before and after each different experimental condition by recording the zero-input response of the airplane to specific initial conditions. The time histories of several pertinent variables were compared visually to a previously recorded standard. These dynamic calibrations, along with the initial

conditions, were also recorded digitally, to help detect any errors in the on-line digital recording equipment.

As stated previously, each session consisted of two experimental conditions. Generally, several days intervened between sessions. Each session lasted approximately two and one half hours, during which thirty separate data runs were made; fifteen at each experimental condition. The subjects were given a break of approximately twenty minutes between the two experimental conditions. They were also given a short break about midway through each block of fifteen runs. The turnaround time between each two-minute run was approximately one minute, during which time the subject was given his relative mean-square tracking error for the previous run.

5.0 DATA AND DATA ANALYSIS

The data resulting from this experiment consisted of two relative mean-square measurements and a digital time history recording for each of the more than 360 runs.

5.1 Mean-Square Tracking Error and Performance Ratio

The relative mean-square altitude deviation and the relative mean-square disturbance input were utilized to determine a performance measure for each run, the Mean Square Tracking Error (MSTE) defined previously in Section 3.0:

$$\text{MSTE} = \frac{\text{mean-square altitude deviation}}{\text{mean-square disturbance input}}$$

Normalization of the mean-square altitude deviation by the noise input reduces the effects of the run-to-run statistical variation of the disturbance input. For each experimental condition of each subject a mean and standard deviation of the 15 MSTE values were calculated.

The data are divided into four groups as follows:

Airplane #1, subject #1

Airplane #2, subject #1

Airplane #1, subject #2

Airplane #2, subject #2

For each of these four conditions, 5 Performance Ratios (PR) were defined as follows:

$$PR = \frac{\text{average MSTE with dynamics}}{\text{average MSTE without dynamics}}$$

This PR is essentially the fractional increase in average MSTE due to the presence of the display dynamics with a particular natural frequency. For example, if the presence of display dynamics did not increase the MSTE for that condition, the PR would be equal to unity. Conversely, if the display dynamics caused twice the mean square altitude deviation, the PR would be equal to 2. These data for each of the four groups are shown in Figure 5.1. The experimental variable on the abscissa is the display dynamics natural frequency, ω_{n_d}. The bars above and below each point represent the 95% confidence level of the mean of the 15 constituent PR's, assuming that the parent population has a normal distribution (Ref 4, pp 243, 244).

Figure 5.1.a shows the results for subject #1 flying airplane #1. For this airplane, on the basis of T tests (Ref 4, p 240), all the differences between the means with display dynamics and the mean without display dynamics are statistically significant at the $P < 0.001$ level except for $\omega_{n_d} = 8.5$ radian/second, which is still significant at the $P < 0.01$ level. Similarly, for subject #2 flying the same airplane (Figure 5.1.b), all the differences between dynamics and no dynamics are significant at the $P < 0.001$ level.

Figure 5.1, c and d show the mean PR's for both subjects controlling aircraft #2. For subject #1, Figure 5.1.c, only the condition for display dynamics at 3 radian/second has differences

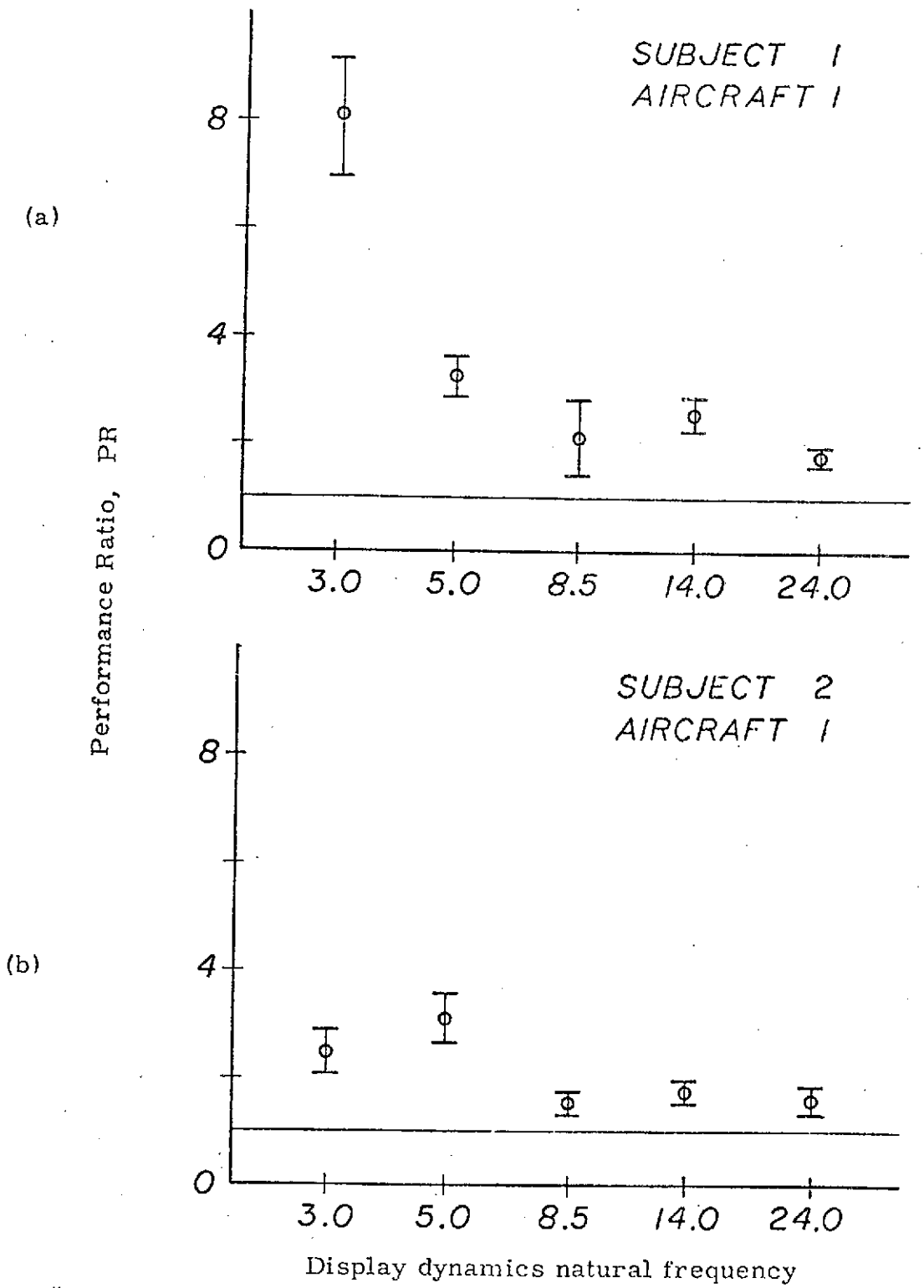

Figure 5.1 Performance Ratio v. s. display dynamics natural frequency for airplane 1

(c)

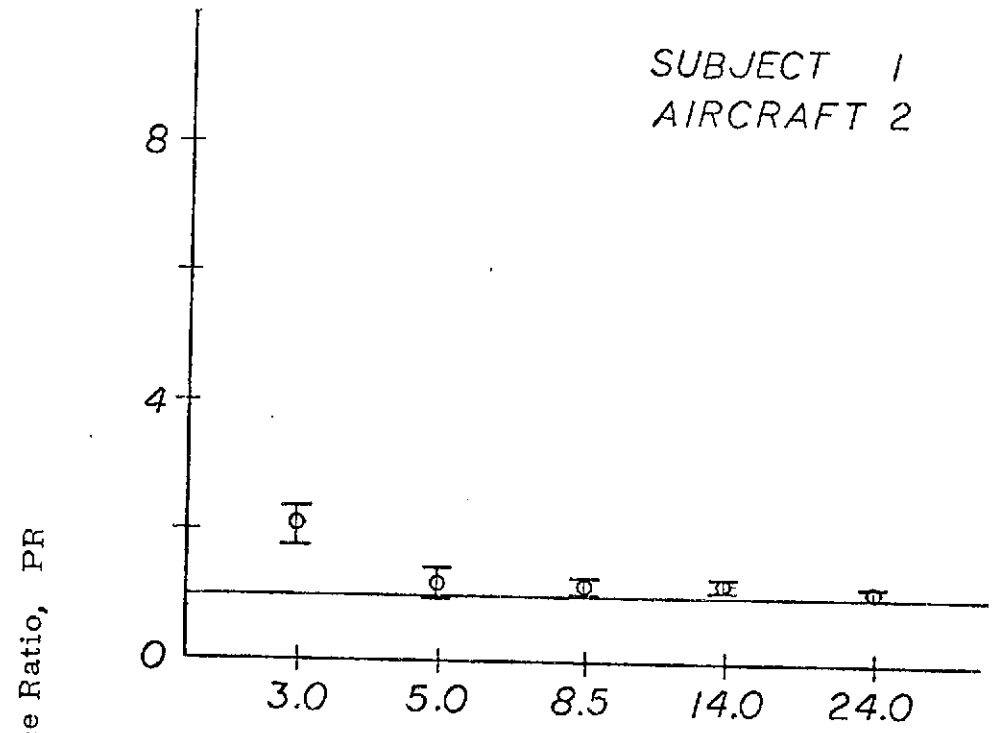

(d)

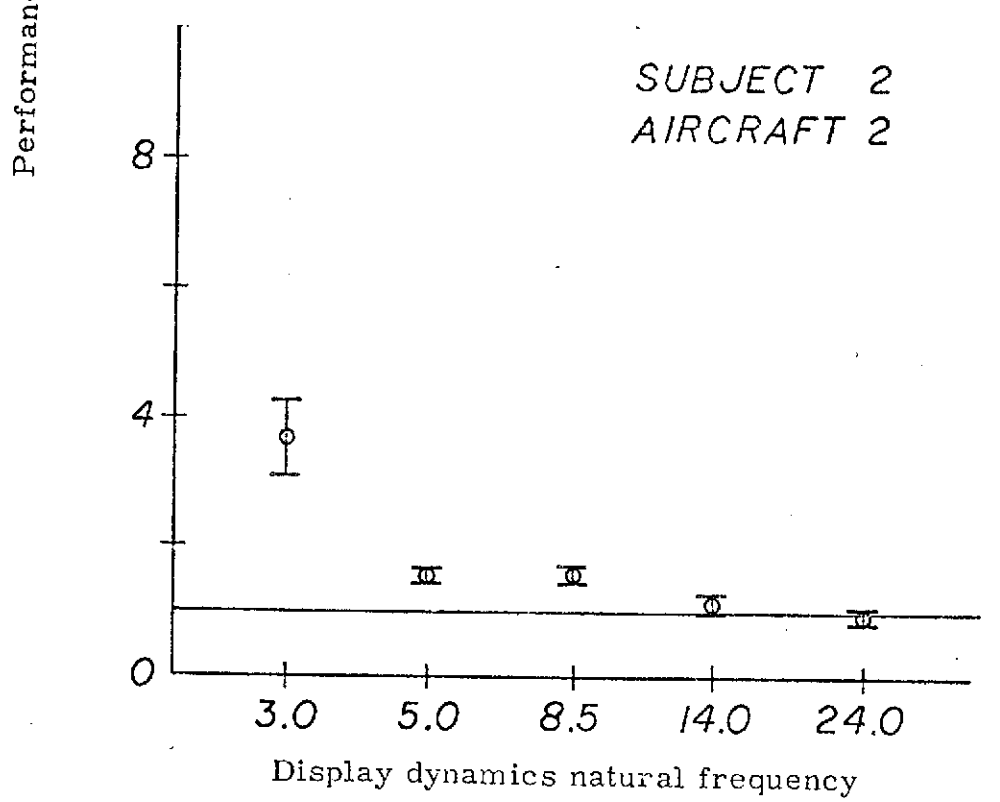

Performance Ratio, PR

Display dynamics natural frequency

Figure 5.1(cont.) Performance Ratio v. s. display dynamics natural frequency for airplane 2

statistically significant at the $P<0.001$ level. Performance differences for the remaining four display dynamics configurations are not statistically significant. For the second subject, same airplane, the first three left hand points, 3.0, 5.0 and 8.5 radian/second, have differences significant at the $P < 0.001$ level. The remaining points are not statistically different from the no dynamics condition.

These data seem to indicate a relationship between the display dynamics natural frequency, the short period natural frequency, and the short period damping ratio of the simulated airplane. This relationship will be discussed further in the following chapter.

5.2 Anomalous Point

The second subject, when controlling airplane #1 with 3 radians/second dynamics, exhibited a level of performance which appeared to be inconsistent with his trends for the other display dynamics and quite different from the performance and trends of the first subject. The PR for the seemingly anomalous point is approximately one fourth the value produced by the other subject. It is also significantly lower than this subject's PR for the adjacent point at 5 radian/second. This point is repeatable. Essentially the same scores were obtained at a session held subsequent to the normal data gathering sessions.

The frequency domain characteristics also show an abrupt change for this condition when compared to other display dynamics for the

same pilot and airplane. Assuming that pitch control is an inner loop, the closed loop transfer function magnitude can be obtained from the relationship

$$|Y_{CL}(j\omega)| = \left[\frac{\Phi_{hh}(\omega)}{\Phi_{nn}(\omega)}\right]^{\frac{1}{2}}$$

where Φ_{hh} and Φ_{nn} are the power spectral density functions for the altitude output and noise input, respectively. Utilizing the time series digital data and a digital frequency analysis program, MIDAS SPECTRAL (Ref 5), power spectral densities for disturbance input and altitude output were generated and used to determine the magnitudes of the closed loop transfer function shown in Figure 5.2. For ω_{n_d} = 3 radian/second, the low frequency gain is much greater than for either of the other two values of ω_{n_d}.

The subjects generally commented that the configurations with low display dynamics frequencies were the most difficult to control satisfactorily. However, for this configuration (ω_{n_d} = 3 radians/second, subject #2, airplane #1) the subject said he felt fairly comfortable flying it and that it was not very difficult to control.

Based on the many differences in the way the second subject controlled this particular configuration, it appears that he adopted an entirely different control philosophy than he exhibited for the other experimental conditions. Because of this apparently different philosophy, the data for this particular condition and subject is not felt to be representative of the performance of a larger population. Consequently, the conclusions drawn from this data will exclude this anomaly.

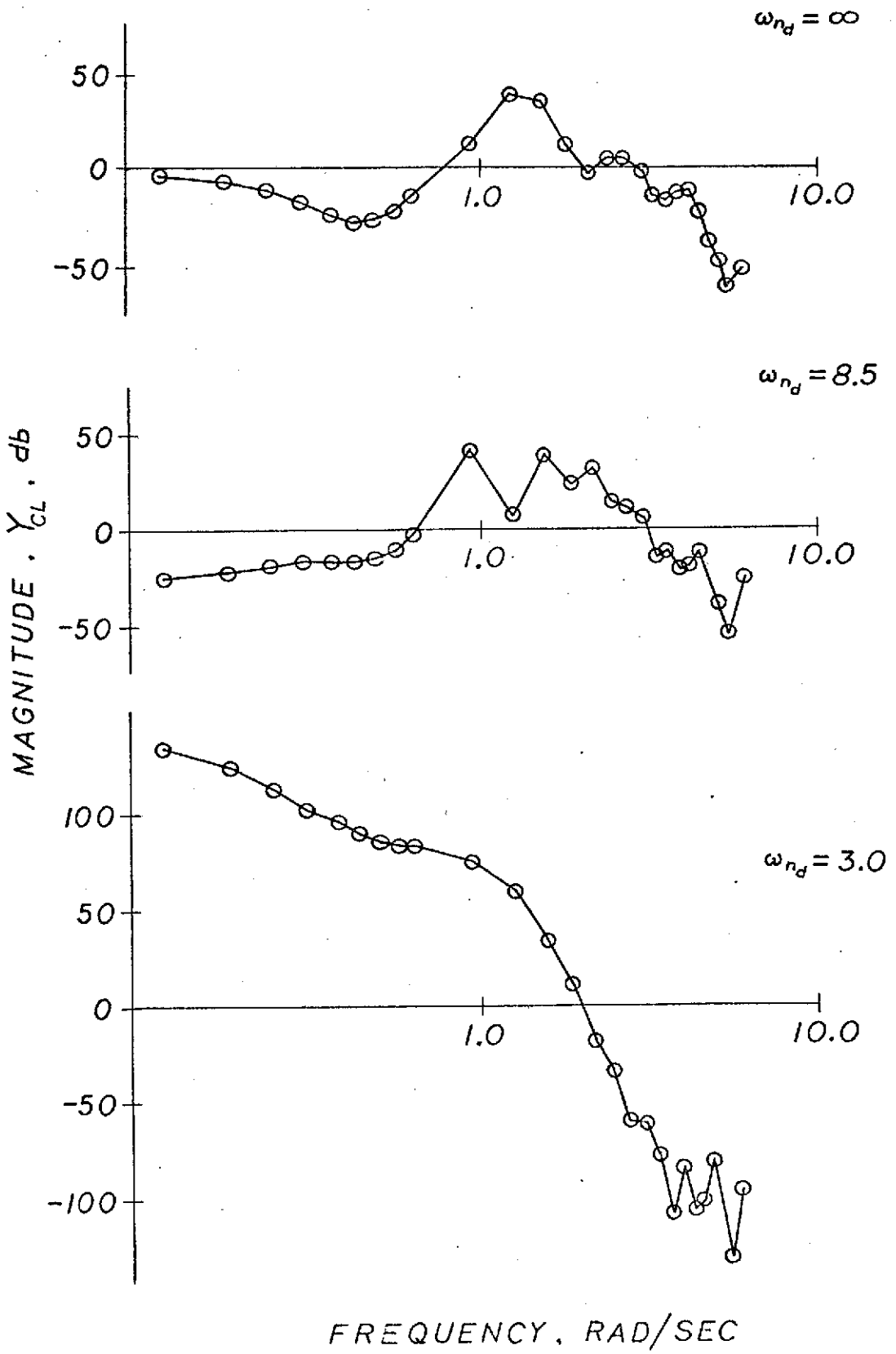

Figure 5.2 Disturbance input to altitude output transfer function magnitude

6.0 CONCLUSIONS AND RECOMMENDATIONS

6.1 Conclusions

The PR's shown in Figure 5.1 of the previous section constitute the major data obtained. These data indicate a relationship between the display dynamics and the short period characteristics of the simulated airplane.

For airplane #1, the airplane with the lower damping ratio, the PR's are substantially higher than for airplane #2. These greater tracking errors are also accompanied by larger intervals for the 95% confidence levels of the means as well as larger standard deviations of the constitutent data. As stated previously, for airplane #1 all the differences between dynamics and no dynamics were statistically significant to the $P < 0.001$ level except one, which was still significant to the $P < 0.01$ level. However, for the more heavily damped airplane, only 4 out of the 10 points were statistically different from the no dynamics baseline. These 4 points were those with the lower display dynamics natural frequencies.

It is informative to examine the various PR values plotted against the ratio of the display dynamics natural frequency to the short-period natural frequency of the simulated aircraft. These data are shown in Figure 6.1. The blocked points represent airplane #1, while the open points represent airplane #2. In general, the data for a particular airplane flown by both subjects seem to group rather well. The means for airplane #1 are generally higher than the means

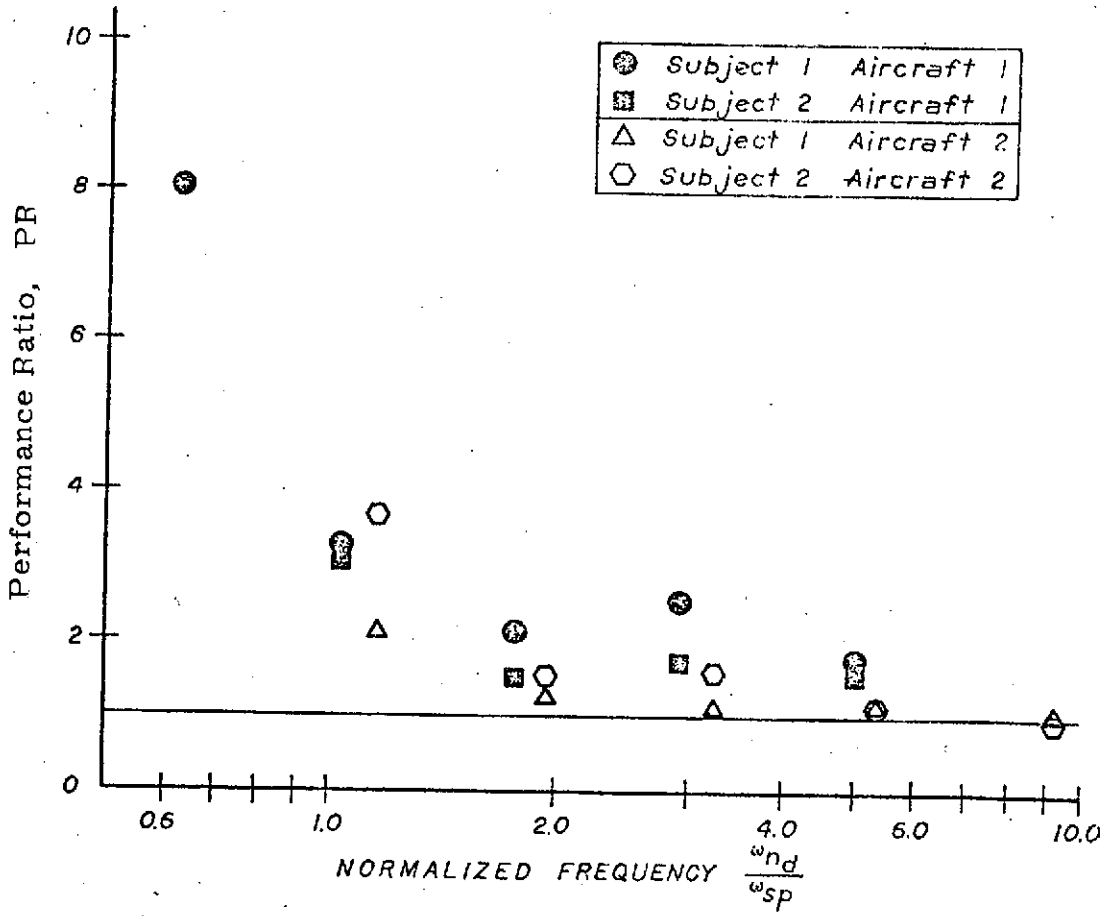

Figure 6.1 Performance ratio v.s. ratio of display dynamics natural frequency to short-period natural frequency

for airplane #2. However, the same type of curve appears to represent the mean data of either set fairly well.

To be more concise, the two conclusions which these data seem to support are these:

1) For this type of altitude tracking task in a fixed base simulator, when the simulated airplane is lightly damped the presence of display dynamics with natural frequencies as high as 5 times the short-period natural frequency causes significant degradation of altitude tracking performance .

2) When the simulated airplane is more heavily damped, the presence of display dynamics is not significant until the ratio of the display dynamics natural frequency to short-period natural frequency is approximately 2 or less.

In summary, whether dynamical display lags will cause degradation of altitude tracking performance depends on both the short period damping ratio and the ratio of the display dynamics natural frequency to the short-period natural frequency of the simulated airplane. The lower the short-period damping ratio, the more the display dynamics will degrade the tracking performance.

6.2 Recommendations for Further Research

The altitude tracking task described in this report is one in which the vertical axis display dynamics are most critical. None the less, it is only one of a large family of tasks and maneuvers for which display dynamic lags may effect the data subsequently obtained in a

flight simulator. A tracking task borders on abstraction since very few situations in real aircraft or flight simulators present this constant type of control requirements. The effects of display dynamics on transient maneuvering motions such as a sudden pitch-up or pitch-down might be even more pronounced than in a tracking task. Further generalizations about the effects of display dynamics can come only from additional experimentation with other types of tracking tasks and, perhaps more importantly, transient maneuvers.

A strong relationship between the tracking errors and the short-period damping ratio is apparent in the data. Additional work is needed to adequately describe and understand this relationship.

Past research concerning turbulence and flying qualities (Ref 6) has shown that turbulence has a strong effect on the over-all closed loop pilot-airplane system performance. Turbulence levels will also affect the display-pilot-simulated-airplane system since the display and its associated dynamics becomes an integral part of the closed-loop system in a flight simulation. It is quite possible that the additional filtering by the display dynamics might result in somewhat different turbulence effects than have been reported for in-flight data.

The results reported herein were generated in a fixed-base simulation. Extrapolation of these data to motion-base simulators must be done cautiously since the dynamical lags present in the

display generation equipment may be substantially different from the lags present in the motion generation mechanisms. Consequently, the pilot may be faced with conflicting or spurious cues, including visual, vestibular, and kinesthetic. Also,the reversal of pilot handling quality opinions between the subjects in this experiment and established in-flight data suggests that the lack of motion cues may have altered their control philosophies. Motion cues cause the phase lead generated by the pilot to be extended to higher frequencies. Since the major degrading influence of the display dynamics appears to be the associated phase lag, the increased human operator phase lead due to motion might well produce better performance, especially with aircraft exhibiting high short-period natural frequencies.

Finally, both the preliminary data and pilot comments indicate that display dynamics can affect pilot performance without the subject being aware of their presence. In many cases, the subjects could not confidently attest to the presence or absence of the display dynamics. Consequently, knowledge of the limits of the pilot's perception of display dynamics might be very useful, since the display dynamics can have a rather insidious influence on the pilot's performance.

APPENDIX A

AIRPLANE EQUATIONS OF MOTION

The aircraft linearized longitudinal equations of motion can be written in the combined wind-axis, body-axis coordinate system as follows (Ref. A 1):

$$\frac{1}{g}\dot{v} = K_{vv}\, v + K_{v\alpha}\,\bar{\alpha} - \gamma + K_{v\alpha}\,\Delta\alpha$$

$$\dot{\bar{\alpha}} = K_{z\alpha}\,\bar{\alpha} + (1 + K_{zq})\, q + K_{z\alpha}\,\Delta\alpha$$

$$\dot{q} = K_{qv}\, v + K_{q\alpha}\,\bar{\alpha} + K_{q\dot{\alpha}}\,\dot{\bar{\alpha}} + K_{qq}\, q + K_{q_{\delta e}}\,\delta e + K_{q\alpha}\,\Delta\alpha + K_{q\dot{\alpha}}\,\dot{\Delta\alpha}$$

$$\dot{\gamma} = q - \dot{\bar{\alpha}}$$

where: $(\dot{\ }) = \dfrac{d(\ )}{dt}$

v = perturbation of total aircraft velocity

$\bar{\alpha}$ = perturbation of angle-of-attack

q = pitch rate (nominal pitch rate = 0)

γ = flight path angle (nominal flight path angle = 0)

and δe, $\Delta\alpha$, and $\Delta\dot{\alpha}$ are forcing functions. These four differential equations can be put into first-order form by appropriate substitution of the $\dot{\bar{\alpha}}$ equation into the right hand side of the $\dot{q}$ and $\dot{\gamma}$ equations. The resulting set of first-order linear differential equations written in vector-matrix form is as follows:

$$\begin{bmatrix} \frac{1}{g}\dot{v} \\ \dot{\alpha} \\ \dot{q} \\ \dot{\gamma} \end{bmatrix} = \begin{bmatrix} gK_{vv} & K_{v\alpha} & 0 & -1 \\ 0 & K_{z\alpha} & 1 + K_{zq} & 0 \\ gK_{qv} & K_{q\alpha} + K_{z\alpha} K_{q\dot{\alpha}} & (1+K_{zq})K_{q\dot{\alpha}} + K_{qq} & 0 \\ 0 & -K_{z\alpha} & -K_{zq} & 0 \end{bmatrix} \begin{bmatrix} \frac{1}{g}v \\ \alpha \\ q \\ \gamma \end{bmatrix}$$

$$+ \begin{bmatrix} 0 & K_{v\alpha} & 0 \\ 0 & K_{z\alpha} & 0 \\ K_{q_{\delta e}} & K_{q\alpha} + K_{z\alpha} K_{q\dot{\alpha}} & K_{q\dot{\alpha}} \\ 0 & -K_{z\alpha} & 0 \end{bmatrix} \begin{bmatrix} \delta e \\ \Delta\alpha \\ \Delta\dot{\alpha} \end{bmatrix}$$

These equations have been simplified by neglecting the following small valued stability derivatives: (Ref A 2)

$$C_{x_{\dot{\alpha}}}, \quad C_{x_q}, \quad C_{x_{\delta e}}$$

$$C_{z_{\dot{\alpha}}}, \quad C_{z_u}, \quad C_{z_{\delta e}}$$

The expressions for the subscripted coefficients, in terms of NACA stability derivatives, are as follows:

$$K_{vv} = \frac{\rho VS}{2mg} C_{x_u}, \quad K_{v\alpha} = \frac{\rho V^2 S}{2mg} C_{x_\alpha}$$

$$K_{z\alpha} = \frac{\rho VS}{2m} C_{z_\alpha}, \quad K_{z_q} = \frac{\rho S c}{4m} C_{z_q}$$

$$K_{qv} = \frac{\rho VSc}{2I_{yy}} C_{m_u}, \quad K_{q_\alpha} = \frac{\rho V^2 Sc}{2I_{yy}} C_{m_\alpha}$$

$$K_{q_{\dot{\alpha}}} = \frac{\rho V S c^2}{4 I_{yy}} C_{m_{\dot{\alpha}}}, \quad K_{qq} = \frac{\rho V S c^2}{4 I_{yy}} C_{m_q}$$

$$K_{q_{\delta e}} = \frac{\rho V^2 S c}{2 I_{yy}} C_{m_{\delta e}}$$

By denoting the state vector as

$$\begin{bmatrix} \frac{1}{g} v \\ \bar{\alpha} \\ q \\ \gamma \end{bmatrix} = \begin{bmatrix} x_1 \\ x_2 \\ x_3 \\ x_4 \end{bmatrix} = X$$

and the control vector as

$$\begin{bmatrix} \delta e \\ \Delta\alpha \\ \Delta\dot{\alpha} \end{bmatrix} = \begin{bmatrix} u_1 \\ u_2 \\ u_3 \end{bmatrix} = U$$

this set of equations can be written in the state-space form

$$\dot{X} = AX + BU$$

$$Y = CX$$

where

$$Y = \begin{bmatrix} y_1 \\ y_2 \end{bmatrix} = \begin{bmatrix} \theta \\ \gamma \end{bmatrix}$$

The numerical values for the A, B, and C matrices are listed in Table A1.

The vertical velocity of the aircraft can be found by $\dot{h} = V \sin \gamma \approx V\gamma$ for small flight path angles. Hence the altitude, h, was determined by

$$h = V \int \gamma \, dt + h_o$$

where h_o is the initial, nominal altitude .

Table A1

Airplane No. 1

$$A_1 = \begin{bmatrix} -0.0134 & -0.490 & 0 & -1.0 \\ 0 & -2.17 & +0.987 & 0 \\ +0.062 & -24.5 & -1.93 & 0 \\ 0 & +1.88 & +0.013 & 0 \end{bmatrix}$$

$$B_1 = \begin{bmatrix} 0 & -0.490 & 0 \\ 0 & -2.17 & 0 \\ -48.0 & -23.0 & -0.363 \\ 0 & +2.17 & 0 \end{bmatrix}$$

$$C_1 = \begin{bmatrix} 0 & 1 & 0 & 1 \\ 0 & 0 & 0 & 1 \end{bmatrix}$$

Airplane No. 2

$$A_2 = \begin{bmatrix} -0.0134 & -0.490 & 0 & -1 \\ 0 & -1.88 & +0.987 & 0 \\ 0.062 & -5.868 & -1.72 & 0 \\ 0 & +1.88 & +0.013 & 0 \end{bmatrix}$$

$$B_2 = \begin{bmatrix} 0 & -0.490 & 0 \\ 0 & -1.88 & 0 \\ -18.6 & -5.87 & -0.363 \\ 0 & +1.88 & 0 \end{bmatrix}$$

$$C_2 = \begin{bmatrix} 0 & 1 & 0 & 1 \\ 0 & 0 & 0 & 1 \end{bmatrix}$$

APPENDIX B

ANALOG-DIGITAL PSEUDO-RANDOM NOISE GENERATION UTILIZING ANALOG FILTERS WITH TWO SEPARATE BREAK FREQUENCIES

The simulated turbulence employed as the disturbance input to the airplane in these experiments was obtained from an analog-digital pseudo-random noise generator. This system consisted of a binary-sequence generator followed by two low-pass filters with break frequencies of 1 radian/second and 10 radians/second respectively. The sequence generator is a clock-driven shift register with the modulo-two sum of the last stage and one other stage fed back to the first stage.

In theory, if the clock frequency, f_c, is greater than three times the filter break frequency, f_b, the output of a binary-sequence generator followed by one or more analog low-pass filters with the same break frequency will be a flat spectrum out to the bandwidth of the analog filters. In practice, however, this is not always the case. Gilson (Ref B1) found that the generator output did not have a gaussian amplitude distribution unless the ratio of clock frequency to filter break frequency, f_c/f_b, was approximately twenty. Figure B 1 shows some of the results of Gilson's investigations of amplitude distributions for various f_c/f_b. When this ratio is too small, the distribution tends to look like two delta functions near the amplitudes of the two input binary logic levels. On the other hand, if this ratio is significantly higher than twenty, the distribution becomes skewed because of the tendency of the binary sequence generator to produce long sequences of predominantly zeroes more

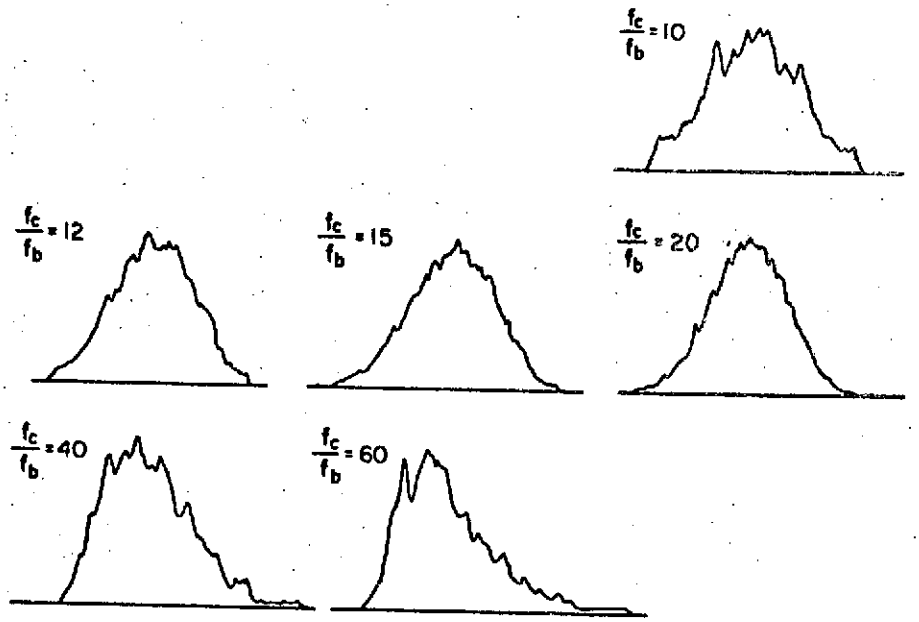

Figure B1 Amplitude distributions for an 11-stage shift register followed by an analog filter with a single break frequency

often than similar long sequences of predominantly ones. A low-pass filter with a suitably long time constant responds more to the strings of zeroes than the strings of ones.

As stated in the first paragraph, the frequency spectrum of the turbulence input employed in this experiment was generated by passing the binary sequence generator output through two first-order low-pass filters with break frequencies of 1 radian/second and 10 radians/second. The available literature considered only the case where the analog filter had a single break frequency. There was no information available which related the amplitude distribution and the clock frequency when there were two break frequencies. This appendix describes the results of an experimental investigation of the relationships between distributions, frequency spectra, and clock frequency for case where the analog filters have two different break frequencies.

The experiment consisted examining the amplitude distributions for several different ratios of clock frequency to first filter break frequency when the analog filter consisted of

$$Y = \frac{10}{(s + 1)(s + 10)}$$

Also, for the most nearly gaussian distribution, the frequency spectrum was computed to determine how closely the output resembled bandwidth limited white noise.

Figure B2 shows the amplitude distributions for clock frequency

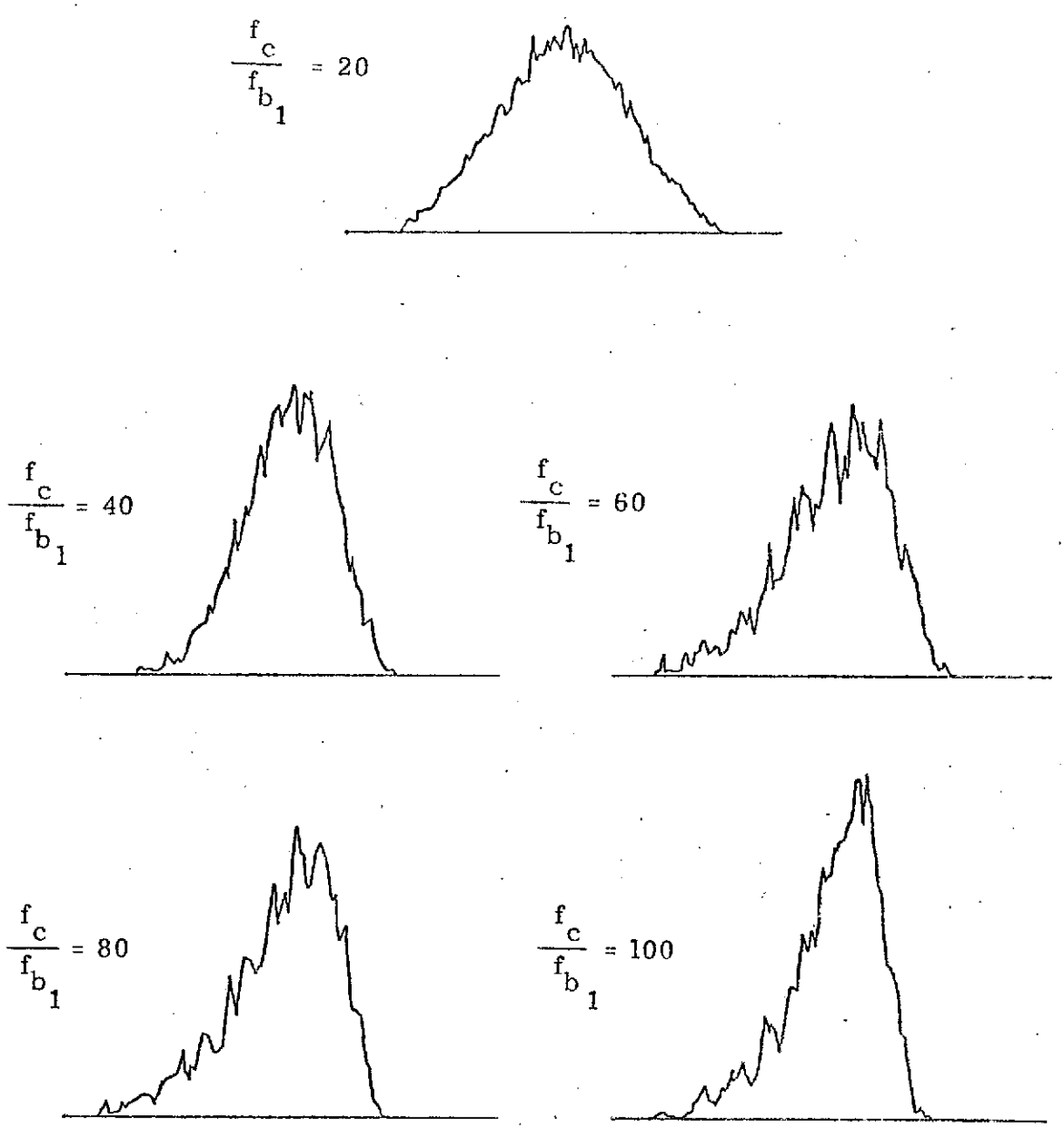

Figure B2 Amplitude distributions for an 11-stage shift register followed by two analog filters with break frequencies a decade apart

to first break frequency ratios $\left(\frac{f_c}{f_{b_1}}\right)$ of 20, 40, 60, 80, and 100. Each distribution represents 14700 discrete data points, or approximately 6 minutes of time history sampled at the rate of 40 samples/second. These results are very similar to those reported by Gilson. Apparently for this particular filter, Gilson's results are applicable if we define the frequency ratio in terms of the lower break frequency, f_c/f_{b_1}. The distribution for $f_c/f_{b_1} = 20$ is reasonably gaussian. However, as this ratio increases, the distributions become increasingly skewed.

For the experiment described in this report, the ratio $f_c/f_{b_1} = 20$ was used for the turbulence spectrum generation. Figure 2.10 shows the power spectral density for this ratio. The data shows good agreement with the desired Dryden spectrum, with sufficient power at the high frequencies.

REFERENCES

1. Barnes, A. G., "The Effect of Visual Threshold on Aircraft Control, with Particular Reference to Approach and Flare Simulation," AIAA Paper No. 70-357, 1970, Presented at the AIAA Visual and Motion Simulation Technology Conf., Cape Canaveral, Fla., March 16-18, 1970.

2. Etkin, B., "Dynamics of Atmospheric Flight," Wiley, New York, 1972.

3. Chalk, C.R., Neal T.P., Harris, T.M., Pritchard, F.E., Woodcock, R.J., "Background Information and User Guide for MIL-F-8785 B (ASG), Military Specification-Flying Qualities of Piloted Airplanes," AFFDL-TR-69-72, August 1969

4. Burington, R.S., May, D.C., "Handbook of Probability and Statistics with Tables," McGraw-Hill, New York, 1970.

5. Fox, D., Guise, K., "Midas, Michigan Interactive Data Analysis System," Statistical Research Laboratory, University of Michigan, 1972.

6. Franklin, J.A., "Turbulence and Longitudinal Flying Qualities," NASA CR-1821, July 1971.

A1. Howe, R.M., "Aircraft Simulation Methods," Dynamics of Flight, Part IV, College of Engineering, University of Michigan, 1956.

A2. Blakelock, J.H., "Automatic Control of Aircraft and Missiles," Wiley, New York, 1965.

B1. Gilson, R. P., "Some Results of Amplitude Distribution Experiments on Shift Register Generated Pseudo-Random Noise," Appendix, Letter Progress Report-Contract No. NASr-54(06), February 1966.